PFG 1/2015, 0021 – 0032
Stuttgart, February 2015

Article

Identification of Agricultural Crop Types in Northern Israel using Multitemporal RapidEye Data

Florian Beyer, Thomas Jarmer & Bastian Siegmann, Osnabrück

Keywords: LU/LC, multitemporal classification, phenology, crops, RapidEye

Summary: Accurate land use / land cover classification (LU/LC) of agricultural crops still represents a major challenge for multispectral remote sensing. In order to obtain reliable classification accuracies on the basis of multispectral satellite data, merging crop classes in rather broad classes is often necessary. With regard to the rising availability and the improving spatial resolution of satellite data, multitemporal analyses become increasingly important for remote sensing investigations. For the separation of spectrally similar crops, multidate satellite images include different growth characteristics during the phenological period. The present study aims at investigating a way to perform highly accurate classifications with numerous agricultural classes using multitemporal RapidEye data. The Jeffries-Matusita separability (JM) was used for applying a pre-procedure in order to find the best multitemporal setting of all available images within one crop cycle, consisting of two cultivation periods P1 with 16 agricultural classes and P2 with 27 agricultural classes. Only one critical class pairing occurred for both P1 and P2 taking into account the best multitemporal dataset. The maximum likelihood (ML) classifier and the support vector machine (SVM) were compared using the most suitable multitemporal images. Both algorithms achieved very high overall accuracies (OAA) of over 90%. SVM was slightly better with a classification accuracy of P1-OAA = 96.13% and P2-OAA = 94.01%. ML provided a result of OAA = 94.83% correctly classified pixels for P1 and OAA = 93.28% for P2. The processing time of ML, however, was significantly shorter compared to SVM, in fact by a factor of five.

Zusammenfassung: *Identifikation landwirtschaftlicher Kulturen in Nordisrael mittels multitemporaler RapidEye-Daten*. Eine hochgenaue Landnutzungsklassifizierung (LU/LC) landwirtschaftlicher Kulturen auf Basis von multispektralen Fernerkundungsdaten stellt noch immer eine große Herausforderung dar. Oftmals müssen unterschiedliche landwirtschaftliche Kulturen zu Oberklassen zusammengefasst werden, damit die Klassifizierung auf Grundlage multispektraler Satellitendaten akzeptable Genauigkeiten erreichen. Mit der steigenden Verfügbarkeit und gleichzeitig verbesserten räumlichen Auflösung von Satellitendaten kommt der multitemporalen Analyse von Fernerkundungsdaten immer mehr Bedeutung zu. Dabei wird der Sachverhalt genutzt, dass verschiedene Pflanzen einen unterschiedlichen phänologischen Verlauf besitzen. Ziel der vorliegenden Studie ist eine hochgenaue Klassifizierung landwirtschaftlicher Flächen mit hoher Klassenanzahl durch die multitemporale Analyse multispektraler RapidEye-Daten. Das Trennbarkeitsmaß Jeffries-Matusita Separability (JM) wurde als Vorverarbeitungsschritt verwendet, um den besten multitemporalen Datensatz aus den verfügbaren einzelnen Aufnahmeterminen eines kompletten Fruchtwechsels, bestehend aus zwei Anbauperioden P1 mit 16 und P2 mit 27 landwirtschaftlichen Klassen, zu finden. Die spektrale Trennbarkeit der vorhandenen Klassen ergab für den ermittelten multitemporalen Datensatz für P1 und P2 nur eine kritische Klassenpaarung. Für die Klassifizierung wurden die Klassifizierungsalgorithmen Maximum Likelihood (ML) und Support Vector Machine (SVM) vergleichend gegenübergestellt. Beide Algorithmen lieferten Gesamtklassifizierungsgenauigkeiten von über 90%. Die SVM erwies sich dabei mit Klassifizierungsgenauigkeiten OAA = 96,13% für P1 und OAA = 94,01% für P2 zwar als geringfügig genauer, jedoch war die ML-Klassifizierung (P1-OAA = 94,83%; P2-OAA = 93,28%) deutlich, d.h. um den Faktor 5, schneller.

www.schweizerbart.de
DOI: 10.1127/pfg/2015/0249
1432-8364/14/0249 $ 3.00

1 Introduction

Information on land use / land cover (LU/LC) forms a crucial data basis in numerous applications for planning, resources management, and identification of environmental changes or ecological forecasting (Khan et al. 2012). Crop identification and monitoring belong to this category (Vicente-Guijalba et al. 2014, Guerschman et al. 2003, Brisco & Brown 1995). Thematic maps of crop types at agricultural field level can provide important information, e.g. to support agricultural policies, to verify the farmers' applications for public subsidies, or assist in the practice of precision agriculture (Alganci et al. 2013). Accurate and up-to-date maps also may form the basis for yield estimates or environmental and land use planning at local, regional, and national levels. Large area mapping of LU/LC from terrestrial survey is, however, very expensive as well as time-intensive. Hence, LU/LC derived from remote sensing data is of utmost importance. Cropland classification is still a major challenge, considering issues like data availability, classification accuracy, operational processing or acquisition costs (Mulla 2013, Lu & Weng 2007). Advantages of satellite images include large area coverage, mainly operational processing and availability of low cost data (Araújo et al. 2011). As a consequence, a multitude of studies on crop type identification using multispectral data have been performed in the past decades (e.g. Mariotto et al. 2013, Cruz-Ramírez et al. 2012, Mathur & Foody 2008, Brisco & Brown 1995, Buechel et al. 1989, Bauer & Cipra 1973). The main problem for detecting crop types using one single multispectral dataset has been the discrimination uncertainty which is caused by variations of many factors, e.g. different phenological stages or varying fractional vegetation cover, shapes and textures (Alganci et al. 2013, Liu et al. 2002). Different vegetation types frequently show very similar spectral behaviour and inner-field spectral variations are often higher than observed between different crop types (Thenkabail et al. 2011, Guerschman et al. 2003). Therefore, most studies used only a few classes or merged crops classes in broader categories (e.g. Guerschman et al. 2003, Brisco & Brown 1995). In order to handle the above-mentioned challenging tasks in LU/LC classifications, phenological information has been investigated by the remote sensing community as an additional dimension in crop identification. As a consequence, numerous studies combined several multispectral Landsat (Wondrade et al. 2014, Demir et al. 2013, Oetter et al. 2001, Lunetta & Balogh 1999) or SPOT datasets (Chust et al. 2004, Murakami et al. 2001) from one growing period and treated them as one single multitemporal scene. Furthermore, the synergism of SAR and multispectral optical satellite data has been evaluated (Vicente-Guijalba et al. 2014, Askne et al. 2013, Waske & van der Linden 2008, Huang et al. 2007, Brisco & Brown 1995). Oetter et al. (2001), for instance, obtained classification accuracies close to 90%, using five Landsat-5 TM images within one year. The considered classes included agricultural crops, orchards, forest and natural cover types as well as urban areas. The subclasses of agriculture finally classified in this study were aggregated to five broader classes instead of the 15 original mapped agricultural categories.

An additional objective in LU/LC classification from remote sensing data is the selection of appropriate classification algorithms. Waske & van der Linden (2008) emphasized the shift from statistical approaches to more powerful and flexible machine learning algorithms for data classification as a recent development in remote sensing. In the past few years many authors compared newly developed and widely established classifiers (Alganci et al. 2013, Mountrakis et al. 2011, Mathur & Foody 2008, Huang et al. 2002 & 2007). However, recent developments of classification algorithms are also associated with an increasing need of computational performance. Considering this assumption, the non-parametric classifier support vector machine (SVM) and the well-known parametric maximum likelihood (ML) classifier were selected and compared regarding the obtained LU/LC classification with respect to overall classification accuracy (OAA) and performance.

Most multitemporal studies classified all possible dataset combinations in order to find the best multitemporal setting/stack. Considering the enormous computational costs

of classifying large-area datasets with many classes and complex algorithms such as SVM, there is a need to perform a pre-classification approach/procedure to accelerate this selection process.

Given the above described background, the major goals of this study were:

1) to investigate the potential of multitemporal RapidEye data for large-scale identification of crops with particular emphasis on accurate spectral separability of numerous different crop types and agricultural classes and
2) to perform a pre-classification procedure in order to find the best multitemporal data setting avoiding long processing times.

2 Study Site and Data

2.1 *Study Site*

The study site (32.5° N, 35.0° E / 32.9° N, 35.3° E) is located in northern Israel and extends from the bay of Haifa to the plain of Jesreel covering an area of 2,500 km^2. The region between Haifa, Nazareth and the Sea of Galilee is one of the main agricultural production areas in Israel. The region is characterized by Mediterranean climate with hot and dry summers as well as rainy cool winters (Singer 2007). Rainfall is limited from September to May with a mean annual precipitation of 539 mm (IMS 2014). Natural conditions in the investigated area allow crop cultivation during two cultivation periods within one year. The first cultivation period (P1) considered for this research lasted from October 2012 to late March 2013. After the crops were harvested, the second cultivation period (P2) started in April and ended in August 2013. During the dry and hot months in summer (May to August) irrigation is quite common.

2.2 *Mapping Land Use / Land Cover*

For each cultivation period a field campaign was conducted. During the first field campaign in March 2013 crops of P1 for 425 agricultural fields were mapped. P1 was characterized by the pluvial period and moderate temperatures during the winter season. Dominant classes were grains (rye and oat) and chickpeas. Smaller fields were mainly cultivated with peas, tomato, different types of cabbage and salads. In total 16 different classes were identified. During the second field survey, crops of P2 were mapped in June 2013 (in total 826 fields). The beginning of P2 coincided with the end of the rainy season. Arid conditions increased during this period from April to August (IMS 2014). As a consequence, farmers have to store and provide water for irrigation. During this cultivation period cotton, watermelon, maize and sorghum were the dominant crops. Compared to P1 much more diverse crop plants were cultivated in P2, such as beetroot, leek, zucchini, pumpkin, muskmelon or different sorts of cabbages and salads. Additionally, non-cultivated fields like fallow, green fallow and grain residues were also considered. Altogether 27 different classes were mapped. After the end of August the weather conditions were not suitable for cultivation any longer except for fruit trees, e.g. avocados, oranges, peaches, or olives.

2.3 *Satellite Data*

The acquisition of RapidEye data was enabled within the RESA project (RESA 597). The data was provided in preprocessing level 3A. Level 3A data include orthorectification with radiometric, geometric and terrain correction (Weichelt et al. 2013). Subsequently, atmospheric correction was conducted with the generic processing chain CATENA developed at DLR (Krauss et al. 2013). Two individual image datasets were available for each cultivation phase (P1: Jan13, Mar13, P2: Jun13, Aug13, Tab. 1). Furthermore, two additional datasets were acquired in October 2012 and April 2013. The October dataset represented the end of the prior arid non-agricultural period and at the same time the beginning of the ongoing first cultivation phase P1. April is the transition period between P1 and P2. Each dataset was a mosaic from two RapidEye tiles (in total 1,000 km^2 per mosaic).

Tab. 1: Datasets used for separability testing.

Cultivation period	Stack names	Acquisition months	Number of datasets (bands)
P1	Oct12	Oct 2012	1 (5)
	Jan13	Jan 2013	1 (5)
	Mar13	Mar 2013	1 (5)
	P1-stack-1	Jan + Mar 2013	2 (10)
	P1-stack-2	Oct 2012 + Jan + Mar 2013	3 (15)
P2	Jun13	Jun 2013	1 (5)
	Aug13	Aug 2013	1 (5)
	P2-stack-1	Jun + Aug 2013	2 (10)
	P2-stack-2	Oct 2012 + Jun + Aug 2013	3 (15)
	P2-stack-3	Oct 2012 + Apr + Jun + Aug 2013	4 (20)

3 Methods

Four agricultural areas representing different natural settings (coastal plain, hilly terrain) in rural and sub-urban environment were selected for mapping. These areas included large scale agriculture as well as small fields with very heterogeneous crop types. A GIS vector layer was created to extract mapped agricultural fields from satellite images. All individual fields were buffered to mask boundary pixels which might represent mixed land use and hence, should be excluded from further processing. The fields mapped during both campaigns (P1 and P2) were divided into a training and a validation dataset. Fields representing in the mean about 25% of the sampled area were used for independent validation. However, depending on availability, the size of the area considered for validation varied by class (about 16% of the area in the minimum (P1: chickpea; P2: leek) and 41% in the maximum (P1: cabbage; P2: zucchini)).

A pre-classification procedure was applied to the mono- and multitemporal RapidEye data to prove which dataset provided the best class separability. In this context, Jeffries-Matusita separability (JM) was calculated for each class pair of P1 and P2. JM is based on a distance calculation between a pair of probability distributions (Thomas et al. 1987). The considered classes had to be normal distributed and hence, small classes such as napa cabbage should be interpreted carefully. Regarding two classes, JM shows a saturating behaviour asymptotically to 2.0, with 0 implying complete similarity and 2 indicating complete separability.

In order to compare each class with each other, the number of possible parings N can be calculated as

$$N = \binom{n}{2} = \frac{n!}{2!(n-2)!} \quad (1)$$

where n is the number of classes.

A well-established operationally-used algorithm ML and a modern machine-learning algorithm SVM were compared regarding their accuracy and performance classifying the crop types. ML and SVM were applied to the datasets which provided best separability results in separability analysis. ML is the most commonly classifier in practice, because of its robustness (Khan et al. 2012, Hall et al. 1995), but often produces 'noisy' results for complex landscapes (Lu & Weng 2007). SVMs are based on statistical learning theory that optimizes separating boundaries between two classes (Sesnie et al. 2010, Vapnik 1999) without requirements such as normal distribution. In the presented study, a radial basis function (with $\gamma = 0.067$ and $C = 100.00$) was selected for SVM parameterization.

In order to assess the performance of both classifiers OAA was calculated. Furthermore, the kappa coefficient κ was determined. κ ranges between 0 and 1, whereas 1 indicates 100% pixels correctly classified.

4 Results and Discussion

4.1 *Spectral Separability*

First, spectral separability was investigated on the basis of the mono- and multitemporal datasets for all classes from P1 and P2. According to (1) there are 120 pairings in P1 and 351 pairings in P2. Pairings are considered to be critical if the JM value was less than 1.9 (Richards 2005). Tab. 2 illustrates the improvement of class separability with increasing temporal and hence, spectral dimension.

The dataset from October 2012 (Oct12) provided the worst separability for P1 with 90 critical pairings of 120 pairings in total. Agricultural fields were fallow at this time, crops mainly not germinated and discrimination between the different land use types, except for different orchard species, was impossible. The second dataset Jan13 represented the mid-position of the phenological development of P1. Many crops were well developed while others were still in early growth stages. Due to the very similar spectral behaviour, the differentiation of several crops was not possible. Hence, 61 of 120 class pairings received JM values below 1.9 indicating limited separability. The third single date was from March 2013 (Mar13) when the mapping campaign was conducted. At this time root crops were already mature and grain crops were at the phenological stage of ears emergence. It was expected that this stage is most appropriate for crop differentiation. Results of the separability analysis confirmed this assumption but the results still show 41 critical pairings (Tab. 2). Tab. 3 (upper part) illustrates the ten worst parings for P1. Considering the spatial resolution of RapidEye with one pixel covering an area of 25 m^2, most of these not clearly separable classes showed a mixed signal of soil and vegetation, which is especially true for green fallow, onions, orchards, fennel and leek. These crops reach their maximum coverage at various times. Therefore, separability of these classes was not satisfying. Obviously separating the different crops just by use of monotemporal multispectral RapidEye image is hardly possible.

As a next step, multitemporal datasets were tested for P1 regarding their feasibility to separate LU/LC classes. Multi-temporal datasets allow considering different growth stages of crops and additional spectral information for class separation. Stacking of two datasets (P1-stack-1: Jan13 and Mar13) including 10 spectral bands already had a tremendous effect on the improvement of spectral separability (Tab. 2) reducing the number of critical pairings to ten. Only the worst pairing (onions and green fallow) showed a JM value of less than 1.7 (1.57, see Tab. 3). The increasing spectral information representing additional temporal information was the essential factor for the improvement.

Tab. 2: Spectral separability of training data for both cultivation period P1 (above), 16 classes, 120 pairings and P2 (below), 27 classes, 351 pairings.

Cultivation period	Stacks	Number datasets	Number classes	Number critical Pairs	Worst pairing (JM)
P1	Oct12	1	16	90	0.3
	Jan13	1	16	61	0.55
	Mar13	1	16	41	0.61
	P1-stack-1	2	16	10	1.57
	P1-stack-2	3	16	1	1.89
P2	Jun13	1	27	126	0.71
	Aug13	1	27	176	0.69
	P2-stack-1	2	27	26	0.51
	P2-stack-2	3	27	9	1.77
	P2-stack-3	4	27	1	1.89

Further on, the Oct12 RapidEye image was included which provided additional spectral information of soils and fallows. Due to strip farming or coarse seeding of many crops, the spectral reflectance was characterized by mixed pixels containing information of soil and plant spectral reflectance, even during the flowering. P1-stack-2 had 15 spectral bands and combined the spectral information of soils from Oct12 with the spectral information of developed plants from Jan13 and Mar13. The additional information on soil reflectance – not included in P1-stack-1 – improved the separability substantially. Only one critical pairing (onions and green fallow, JM = 1.884) remained with a JM value close to 1.9. The typical spectral reflectance of both classes was made up by mixed pixels containing a high portion of soil reflectance due to the onions planted in lines leaving uncovered soil in between on one hand and the successional character of green fallow resulting in a very heterogeneous soil-influenced spectral behaviour on the other hand. Tab. 3 illustrates the improvement of separability with stacking additional datasets but it is clearly visible, that only the soil information yielded JM-values over 1.9, except for onions and green fallow.

Monotemporal datasets separability analysis for P2 (Tab. 2) provided more critical pairings compared to P1. The main reason was the much higher number of classes during this cultivation period. The monotemporal dataset Jun13 represented the month in which the

Tab. 3: The ten worst parings with JM values (bad separability < 1.8 (red); 1.8 – 1.9 moderate separability (yellow); good separability > 1.9 (green), 2 complete separability) for all mono- and multitemporal datasets in P1 and P2.

		Critical pairings		Oct12	Jan13	Mar13	P1-stack-1	P1-stack-2
P1	1	Green fallow	Onion	0.304	0.551	0.614	1.575	1.887
	2	Green fallow	Chickpeas	0.546	0.634	0.775	1.789	1.935
	3	Green fallow	Orchard	0.547	0.661	1.107	1.813	1.943
	4	Chickpeas	Orchard	0.604	0.831	1.125	1.848	1.948
	5	Peas	Pastureland	0.636	0.833	1.187	1.859	1.960
	6	Chickpeas	Onion	0.684	0.867	1.198	1.860	1.969
	7	Peas	Green fallow	0.699	1.049	1.281	1.880	1.972
	8	Grain	Millet	0.715	1.074	1.338	1.890	1.974
	9	Leek	Onion	0.734	1.177	1.375	1.890	1.977
	10	Fennel	Orchard	0.738	1.229	1.474	1.894	1.982
				Jun13	Aug13	P2-stack-1	P2-stack-2	P2-stack-3
P2	1	Green fallow	Grain residues	0.705	0.690	1.514	1.773	1.890
	2	Green fallow	Orchard	0.792	0.708	1.552	1.812	1.928
	3	Pumpkin	Watermelon	0.801	0.708	1.664	1.838	1.949
	4	Fallow	Grain residues	0.883	0.748	1.700	1.844	1.951
	5	Muskmelon	Watermelon	0.925	0.791	1.709	1.847	1.975
	6	Muskmelon	Pumpkin	1.007	0.858	1.715	1.868	1.978
	7	Maize	Sorghum	1.020	0.862	1.724	1.873	1.979
	8	Muskmelon	Onion	1.115	0.868	1.725	1.875	1.982
	9	Onion	Pumpkin	1.139	0.914	1.729	1.888	1.988
	10	Tomato	Watermelon	1.142	0.968	1.732	1.919	1.989

mapping campaign was conducted. The beginning of June was very appropriate for mapping because root crops were almost mature and easy to distinguish. The number of critical pairings in Jun13 (126) was lower than for Aug13 (176). In Aug13 the crops were mostly harvested, except late crops like maize, sorghum, and cotton.

Tab. 2 indicates a substantial improvement for P2-stack-1 (June and August 2013) in comparison to monotemporal analysis. From more than 100 critical pairings for the monotemporal datasets, critical pairings dropped to 26. However, the worst pairing green fallow and grain residues had still a very low JM value (0.51). Analogous to P1, the October 2012 dataset was used in P2-stack-2 as additional spectral soil/fallow information. Separability test for P2-stack-2 provided crucial improvements. Of 351 parings only nine were critical (Tab. 3) and even the worst pairing showed a high JM value (1.77).

Tab. 3 (lower part) illustrates the ten worst pairings of all 351 in P2. It is remarkable that watermelons, muskmelons and pumpkins appeared most frequently. All those classes belong to the same botanic family (Cucurbitaceae). At the beginning of plant development the physiognomy of these crops is very similar. As a consequence, these crop types show almost identical spectral reflectance and separation was not feasible. This is well in line with Tigges et al. (2013) who confirmed for multispectral data, that only multitemporal analyses allow distinguishing plants in deeper levels of the botanical taxonomy. A similar observation applies for maize and sorghum which physiognomies are relatively homogenous except for the blossoms and the corncob. These crop types were only separable through the temporal information. Green fallow and grain residues as well as green fallow and orchards appeared as the two worst parings which can be explained by mixed pixels of soil and plant signal. These classes are characterized by very heterogeneous inner-field variations and Tab. 3 indicates that the problem was only solved by adding the soil information from October 2012 (Oct 12).

In order to separate the nine remained pairings, Apr13 was included as an additional dataset for P2. The dataset was acquired on 24th April 2013. At this time harvesting during P1 was completed and plant growth of P2 started for allowing the detection of initial spectral signals of vegetation in the satellite data. P2-stack-3 (Oct12, Apr13, Jun13 and Aug13) including 20 spectral bands provided the best separability for P2. Only green fallow and grain residual remained as a critical pairing. Nevertheless, the JM value of 1.89 still suggested a very high quality of separability.

Tab. 4: Accuracy assessment of ML and SVM for both cultivation periods (t(h) = processing time in hours (OAA = overall accuracy in %)).

Cultivation period		P1	P2
Stacks		P1-stack-2	P2-stack-3
Class No.		16	27
ML	OAA	94.83	93.28
	K	0.93	0.92
	t(h)	5	14
SVM	OAA	96.13	94.01
	K	0.95	0.93
	t(h)	27	82

4.2 *Classification*

The stacks P1-stack-2 and P2-stack-3 showed the best spectral separability for the cultivation periods. Therefore, these multitemporal datasets were selected for both classifiers ML and SVM. The training dataset was used to calibrate ML and SVM and the classifications were applied to the entire mosaics consisting of two RapidEye tiles (1,000 km^2). In order to validate the results, the validation dataset was used to determine OAA and κ. Tab. 4 illustrates the validation results for the performed classifications. OAA and κ indicated very high classification accuracies for both algorithms. 94.83% were classified correctly with ML in P1 and a κ of 0.93 indicated a very robust and highly accurate classification.

With an OAA of 96.13% and κ = 0.95 the SVM provided a slightly higher accuracy, suggesting that SVM was better suited to handle higher dimensional data than ML. The same tendency was observed for P2. Even with 27 classes, the SVM classification accuracy was

far above 90% (94.01%) with κ of 0.93 pointing at very robust classification results (ML: OAA = 93.28%; κ = 0.92). However, besides the classification accuracy, the performance of both classifiers was considered. In comparison to ML the processing time (t in hours) increased about a factor of 5 or 6 for SVM. As a consequence, SVM classification of P2 took 3.5 days for the 27 classes. At least regarding the presented study a slight increase in classification accuracy has to be weighed against a substantial increase in processing time.

According to the separability tests, the Jun13 dataset would allow the best classification result of all monotemporal datasets in P2. Consequently, ML and SVM classification were applied additionally to this dataset to allow a comparison of mono- and multitemporal datasets in the spatial domain.

Fig. 1 compares the mapping of P2 with ML and SVM classifications from Jun13 and P2-stack-3 (best multitemporal separability) for a part of the study site. The Jun13 ML classification provided an OAA of 66.94% (κ = 0.63) while the monotemporal SVM classification at least could classify the Jun13 dataset with an OAA of 77.18% (κ = 0.74). Obviously, for both classifiers a tremendous increase in classification accuracy was achieved using multi- instead of monotemporal datasets. Guerschman et al. 2003 obtained similar results, but only after merging nine agricultural classes to four broader classes.

Lu & Weng (2007) emphasized the 'noisy' results for ML classifications. This is clearly visible for the monotemporal ML classification in Fig. 1. Furthermore, a lot of additional misidentified classes appear in both monotem-

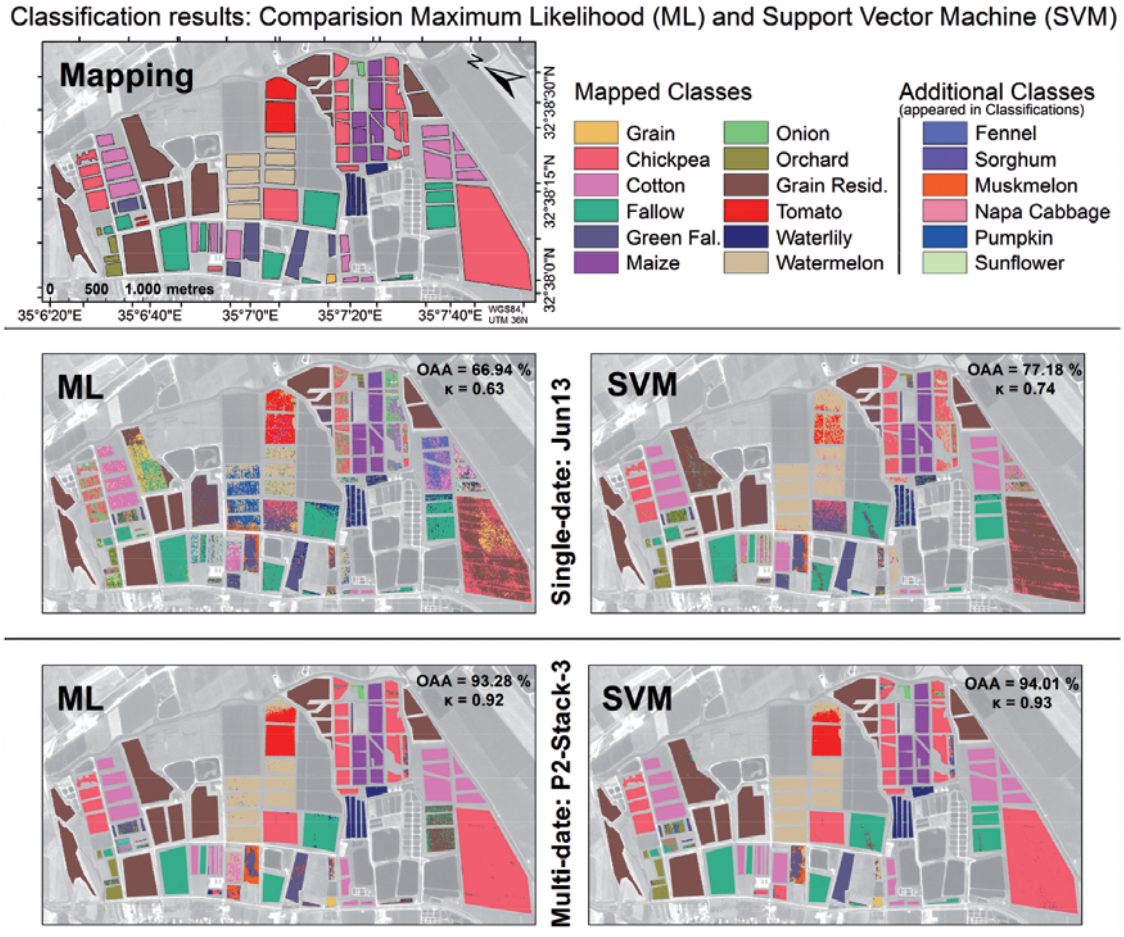

Fig. 1: Comparison of ML and SVM Classification for a monotemporal dataset of June 2013 (Jun13) and a multitemporal dataset (P2-stack-3) for a part of the study site.

poral classifications ML and SVM. These classes occurred in the classification of the entire study site but not in the presented subset in Fig. 1. Regarding the large chickpeas field (Fig. 1 rose) in the south, ML was not able to distinguish between chickpeas, grain residues or grains based on the monotemporal image. The SVM in the monotemporal image mostly identified this field as grain residues. In general, chickpeas fields have spectrally a very high inner-field variation and in June the plants were already dried out. Hence, the classifiers could not differentiate between dried grains and dried chickpeas in the single June dataset. The multitemporal classifications, in contrast, showed highly accurate classification results. This refers to additional phenological information, e.g. the signal of young plants in April and the longer lasting growing period at the end of P2, which was helpful to correctly identify chickpeas.

The same applies to the cotton fields in Fig. 1 (pink), especially in the neighbourhood of the already mentioned chickpea field. ML on monotemporal data identified fennel, waterlily, sunflower and other classes instead of cotton. Due to the dry and hot climate conditions in June (Singer 2007) cotton fields need to be irrigated. Furthermore, cotton was cultivated in stripes. Consequently a RapidEye pixel of 25 m^2 contains a mixed signal of soil (dry and irrigated) and plant (cotton). The result of the SVM in this case was slightly better, but only for the multitemporal dataset almost all pixels of the cotton fields were classified correctly. Again, the multitemporal information was the determining factor for crop differentiation. The harvested fields with crop residues (Fig. 1 brown) were classified very precisely except for one field in the north. This field was still covered by a lot of straw during field survey and hence, ML classified most pixels as grains. In general, the P2 mapping contains only a few fields with mature and dry grains. Only the temporal information allowed the separation between unharvested grains and the field with a high amount of grain residues.

Considering only the two multitemporal classifications in Fig. 1, results were very similar, except one fallow in the south of the water reservoirs. The ML of P2-stack-3 was identifying a lot of pixels of this field as grain residues. The classification of the watermelon fields (Fig. 1 crème) was slightly better using the SVM, because the ML identified some pixels as pumpkin. Pumpkins and watermelons are from the same botanic family (Cucurbitaceae) and have a similar appearance at the beginning of the growing season. Especially the ML classification for the monotemporal image showed a strong mixture between these root crops. The multitemporal classifications contain almost no misidentified classes.

5 Conclusions and Outlook

The present study confirmed the assumption that multispectral satellite data have great potential for multitemporal LU/LC mapping of numerous different agricultural classes with high accuracies. RapidEye data are not only convenient from the spatial point of view (5 m GSD, 79 km swath width), but also from radiometry the increased spectral information of multi-date stacks play an important role for crop differentiation. The JM separability was proven as a very useful pre-testing method to find the best stack combination for the spectral separation of different LU/LC classes. For the first cultivation period (P1) with 16 classes and thus 120 class pairings a multi-date stack of three datasets was used to separate almost all classes. Only one pairing remained closely under the threshold. However, the classifications provided accuracies over 90% for both selected classifiers (ML 94.83% and SVM 96.13%). The same applies to the second period (P2). The class separability was incrementally improved by stacking RapidEye tiles of different dates during the growing season. 27 classes were separated with a multi-date dataset of four stacked RapidEye images. Both classification results supported the assumption that multitemporal datasets provide higher potential in LU/LC classification with overall accuracies over 90% (ML 93.28%, SVM 94.01%). SVM showed its suitability for spectral data with higher dimension while ML provided slightly lower classification accuracies for both periods. However, considering the performance, ML classified the entire dataset with about 1,000 km^2 much faster than SVM (by a factor of 5).

The study has demonstrated that stepwise integration of datasets improved the spectral separability between different classes and hence, the classification accuracies. It is expected that additional datasets from the remaining, non-acquired months lead to even better results. The weather conditions for the region of northern Israel are very suitable for optical remote sensing considering cloud coverage. The RapidEye satellites, in addition, have convenient orbit track geometry to acquire the entire study site in one or two overpasses. Therefore, a monthly or a 14 days acquisition cycle should have additional positive effects. The missing months were November, December and February for P1. Especially a February dataset from 2013 would be helpful to consider the development of root crops. Analogous to the April dataset of P2, additional November and December images of 2012 are assumed as helpful to account for different initial phases of crop growth during P1. Covering the entire first cultivation period may allow separating extremely similar crops as well as even different grain types (oat, rye and barley).

The same applies to the missing months May, July and September of P2. A May 2013 image containing spectral information about vegetation at early growing stages would have been preferred over an April 2013 image ensuring that no reflectance of very late crops by chance is included in the classification. Moreover, July as a mid-position of the phenological period may improve the critical separation of some class pairings, such as green fallow and onions. In order to consider late mature crops, a September dataset would have been helpful.

In summary, multitemporal analyses of the complete crop cycle may be improved with a monthly availability of RapidEye or similar optical remote sensing data. In this case, the issue of the most important datasets for crop identification could be investigated allowing the development of a temporally optimized and even more operational procedure.

Acknowledgements

The authors want to thank the German Aerospace Center (DLR), RESA Science Team, Neustrelitz for the support by providing the satellite data of the RapidEye Science Archive (proposal no. 597). We also thank the staff of the DLR (Oberpfaffenhofen), namely Thomas Krauss and Peter Fischer, for the atmospheric correction using the generic processing chain CATENA. The joint research project "Inference of Aerosol and Land Use Interactions from Remote Sensing Data" (AerosolLand, ZN2725 11-76251-99-20/11) was financially supported by the State of Lower-Saxony, Hannover, Germany.

References

Alganci, U., Sertel, E., Ozdogan, M. & Ormeci, C., 2013: Parcel-level identification of crop types using different classification algorithms and multi-resolution imagery in southeastern turkey. – Photogrammetric Engineering and Remote Sensing **79** (11): 1053–1065.

Araújo, G.K.D., Rocha, J.V., Lamparelli, R.A.C. & Rocha, A.M., 2011: Mapping of summer crops in the state of Paraná, Brazil, through the 10-day spot vegetation NDVI composites. – Engenharia Agrícola **2** (4): 760–770.

Askne, J.I., Fransson, J.E., Santoro, M., Soja, M.J. & Ulander, L.M., 2013: Model-based biomass estimation of a semi-boreal forest from multitemporal tandem-x acquisitions. – Remote Sensing **5** (11): 5574–5597.

Bauer, M.E. & Cipra, J.E., 1973: Identification of agricultural crops by computer processing of ERTS MSS data. – Technical Report 030173, LARS, Perdue University, IN, USA.

Brisco, B. & Brown, R., 1995: Multidate sar/tm synergism for crop classification in Western Canada. – Photogrammetric Engineering & Remote Sensing **61** (8): 1009–1014.

Buechel, S.W., Philipson, W.R. & Philpot, W.D., 1989: The effects of a complex environment on crop separability with Landsat TM. – Remote Sensing of Environment **27** (3): 261–271.

Chust, G., Ducrot, D. & Pretus, J.L., 2004: Land cover discrimination potential of radar multitemporal series and optical multispectral images in a Mediterranean cultural landscape. – International Journal of Remote Sensing **25** (17): 3513–3528.

Cruz-Ramírez, M., Hervás-Martínez, C., Jurado-Expósito, M. & López-Granados, F., 2012: A multi-objective neural network based method for cover crop identification from remote sensed data. – Expert Systems with Applications **39** (11): 10038–10048.

Demir, B., Bovolo, F. & Bruzzone, L., 2013: Classification of time series of multispectral images with limited training data. – IEEE Transactions on Image Processing **22** (8): 3219–3233.

Guerschman, J.P., Paruelo, J.M., Bella, C.D., Giallorenzi, M.C. & Pacin, F., 2003: Land cover classification in the Argentine pampas using multi-temporal Landsat tm data. – International Journal of Remote Sensing **24** (17): 3381–3402.

Hall, F.G., Townshed, J.R. & Engman, E.T., 1995: Status of Remote Sensing Algorithms for Estimation of Land Surface State Parameters. – Remote Sensing of Environment **51** (1): 138–156.

Huang, C., Davis, L.S. & Townshend, J.R.G., 2002: An assessment of support vector machines for land cover classification. – International Journal of Remote Sensing **23** (4): 725–749.

Huang, H., Legarsky, J. & Othman, M., 2007: Land-cover classification using Radarsat and Landsat imagery for St. Louis, Missouri. – Photogrammetric Engineering and Remote Sensing **73** (1): 37–43.

IMS, 2014: Israeli Metereological Survey. – http://www.ims.gov.il (1.3.2014).

Khan, G.A., Khan, S.A., Zafar, N.A., Ahmad, F. & Islam, S., 2012: A review of different approaches of land cover mapping. – Life Sciences Journal **9** (4): 1023–1032.

Krauss, T., d'Angelo, P., Schneider, M. & Gstaiger, V., 2013: The Fully Automatic Optical Processing System CATENA at DLR. – ISPRS International Archives of Photogrammetry Remote Sensing Spatial Information Science **XL-1/W:** 177–181, Copernicus Publications, ISPRS Hannover Workshop 2013.

Liu, Q.J., Takamura, T., Takeuchi, N. & Shao, G., 2002: Mapping of boreal vegetation of a temperate mountain in China by multitemporal Landsat tm imagery. – International Journal of Remote Sensing **23** (17): 3385–3405.

Lu, D. & Weng, Q., 2007: A survey of image classification methods and techniques for improving classification performance. – International Journal of Remote Sensing **28** (5): 823–870.

Lunetta, R.S. & Balogh, M.E., 1999: Application of multi-temporal Landsat 5 tm imagery for wetland identification. – Photogrammetric Engineering and Remote Sensing **65** (11): 1303–1310.

Mariotto, I., Thenkabail, P.S., Huete, A., Slonecker, E.T. & Platonov, A., 2013: Hyperspectral versus multispectral crop-productivity modeling and type discrimination for the hyspiri mission. – Remote Sensing of Environment **139:** 291–305.

Mathur, A. & Foody, G.M., 2008: Crop classification by support vector machine with intelligently selected training data for an operational application. – International Journal of Remote Sensing **29** (8): 2227–2240.

Mountrakis, G., Im, J. & Ogole, C., 2011: Support vector machines in remote sensing: A review. – ISPRS Journal of Photogrammetry and Remote Sensing **66** (3): 247–259.

Mulla, D.J., 2013: Twenty five years of remote sensing in precision agriculture: Key advances and remaining knowledge gaps. – Biosystems Engineering **114** (4): 358–371, Special Issue: Sensing Technologies for Sustainable Agriculture.

Murakami, T., Ogawa, S., Ishitsuka, N., Kumagai, K. & Saito, G., 2001: Crop discrimination with multitemporal spot/hrv data in the Saga plains, Japan. – International Journal of Remote Sensing **22** (7): 1335–1348.

Oetter, D.R., Cohen, W.B., Berterretche, M., Maiersperger, T.K. & Kennedy, R.E., 2001: Land cover mapping in an agricultural setting using multiseasonal thematic mapper data. – Remote Sensing of Environment **76** (2): 139–155.

Richards, J., 2005: Analysis of remotely sensed data: the formative decades and the future. – IEEE Transactions on Geoscience and Remote Sensing **43** (3): 422–432.

Sesnie, S.E., Finegan, B., Gessler, P.E., Thessler, S., Bendana, Z.R. & Smith, A.M.S., 2010: The multispectral separability of costa rican rainforest types with support vector machines and random forest decision trees. – International Journal of Remote Sensing **31** (11): 2885–2909.

Singer, A., 2007: The Soils of Israel. – 306 p., Springer, Berlin, Heidelberg.

Tigges, J., Lakes, T. & Hostert, P., 2013: Urban vegetation classification: Benefits of multitemporal RapidEye satellite data. – Remote Sensing of Environment **136:** 66–75.

Thenkabail, P.S., Lyon, J.G. & Huete, A., 2010: Hyperspectral remote sensing of vegetation and agricultural crops: knowledge gain and knowledge gap after 40 years of research. Ch. 28. – Thenkabail, P.S., Lyon, J.G. & Huete, A. (eds.), 2011: Hyperspectral Remote Sensing of Vegetation. – 705 p., CRC Press, Boca Raton, FL, USA.

Thomas, I.L., Ching, N.P., Benning, V.M. & D'Aguanno, J.A., 1987: Review article a review of multi-channel indices of class separability. – International Journal of Remote Sensing **8** (3): 331–350.

Vapnik, V.N., 1999: An Overview of Statistical Learning Theory. – IEEE Transactions on neural networks **10** (5): 988–999.

Vicente-Guijalba, F., Martinez-Marin, T. & Lopez-Sanchez, J., 2014: Crop phenology estimation using a multitemporal model and a Kalman filtering strategy. – IEEE Geoscience and Remote Sensing Letters **11** (6): 1081–1085.

Waske, B. & van der Linden, S., 2008: Classifying multilevel imagery from sar and optical sensors by decision fusion. – IEEE Transactions on Geoscience and Remote Sensing **46** (5): 1457–1466.

Weichelt, H., Rosso, P., Marx, A., Reigber, S., Douglass, K. & Heynen, M., 2013: The RapidEye red edge band. – Technical report, BlackBridge, Berlin.

Wondrade, N., Ostein, B.D. & Tveite, H., 2014: Gis based mapping of land cover changes utilizing multi-temporal remotely sensed image data in lake Hawassa watershed, Ethiopia. – Environmental Monitoring and Assessment **186** (3): 1765–1780.

Address of the Authors:

Florian Beyer, Dr. Thomas Jarmer & Bastian Siegmann, Institute for Geoinformatics and Remote Sensing, Osnabrück University, Barbarastr. 22b, D-49076 Osnabrück, Tel.: +49-541-969-3930, Fax: +49-541-9693939, e-mail: {fbeyer}{tjarmer}{bsiegmann}@igf.uos.de

Manuskript eingereicht: April 2014
Angenommen: Juli 2014